e-ISSN: 2805-5756

PENERBIT PRESS
UNIVERSITI TEKNOLOGI MARA

Available online at
https:// jaeds.uitm.edu.my

Journal of Applied Engineering Design and Simulation 6(2) 2026, 130-145

Journal of Applied Engineering Design and Simulation

Numerical evaluation of hydraulic performance of a laboratory-scale Archimedes screw pump

Nelson Lee Teck Hua[1], Muhammad Noor Afiq Witri Muhammad Yazid[1*], Muhammed Amirul Asyraf Hasnan[1]

[1] *Faculty of Mechanical Engineering, Universiti Teknologi Malaysia, 81310 Johor Bahru, Johor, Malaysia*

ARTICLE INFO

Article history:
Received 6 August 2026
Revised 27 September 2026
Accepted 6 October 2026
Online first 15 October 2026
Published 15 October 2026

Keywords:
Archimedes screw pump
Hydraulic performance
Inclination angle
Rotational speed
Computational fluid dynamics

DOI:
10.24191/jaeds.v6i2.211

ABSTRACT

Archimedes screw pump (ASP) is a type of positive displacement pump for transporting water from lower to upper incline elevations. It is a simple and robust pump widely used for irrigation, flood mitigation, and in wastewater treatment plants. Although ASPs have been used for centuries, there is a lack of literature related to the optimal hydraulic performance and elucidating the underlying flow mechanisms. This study focuses on numerically evaluating ASP hydraulic performance across various rotational speeds and inclination angles. Experiments have also been performed on a laboratory-scale ASP with three flights, a length of 1500 mm, and an outer diameter of 300 mm for CFD validation. A computational fluid dynamics (CFD) model was developed to replicate the experimental setup, performed using the *k-ε* turbulence model with sliding mesh and the volume of fluid (VOF) method, which is suitable for liquid flow modeling involving combined free surface flow and rotational motion. The CFD model of ASP was simulated under various rotational speeds (25, 50, 75, and 100 rpm) and inclination angles (20°, 25°, and 30°). The results showed that flow rate and torque increase when rotational speed increases for all inclination angles. A maximum efficiency of 94.4% was obtained at 50 rpm and an inclination angle of 30°. These findings provide a useful reference for identifying optimal hydraulic performance of ASP using a CFD-based framework.

Nomenclature

β	Inclination angle (°)
ω	Rotational speed (rpm)

[1*]Corresponding author. *E-mail address*: mnafiqwitri@utm.my

k	Turbulent kinetic energy (m^2/s^2)
ε	Turbulent dissipation rate (m^2/s^3)
ρ	Density (kg/m^3)
g	Gravitational force(m/s^2)
η	Hydraulic efficiency (%)
D_i	Inner diameter (mm)
D_o	Outer diameter (mm)
H	Head (mm)
h_U	Upper water level (m)
h_L	Lower water levels (m)
Gw	Gap width (mm)
L	Length (mm)
N	Number of flight (-)
S	Pitch length (mm)
P_m	Motor power (W)
P_h	Hydraulic power (W)
T	Torque (N·m)
Q	Volume flow rate (m^3/s or L/s)
t	Flight thickness (mm)
Z_{wl}	Bucket water level (m)
TP	Touch point (mm)
FP	Filling point (mm)
CP	Chute point (mm)

Abbreviations

ASP	Archimedes screw pump
AST	Archimedes screw turbine
CFD	Computational fluid dynamics
VOF	Volume of fluid
BCE	Before common era
IFM	Integrated flood management
SIMPLE	Semi-implicit method for pressure-linked equations
PRESTO!	Pressure staggering option
ANSYS	Analysis Systems

1. INTRODUCTION

Archimedes screw pump (ASP) is the oldest type of pump used to transport fluid. It is the earliest hydraulic machine, which was established in the third century BCE and named after the Greek mathematician Archimedes in Egypt [1]. Archimedes invented it as a water screw for irrigation fields and for pumping water out of mines and ship holds [2]. A review paper by Hoofstaedt et al. [3] highlighted that Archimedes screws can operate effectively at low heads. Given the system's ability to handle dirty or debris-laden water, another application of ASP is to improve the drainage of flood areas [4]. Aside from flood mitigation, a recent study by Llave-Propín et al. [5] found that the Archimedes screw is a fish-friendly pump to transfer fish compared to a vacuum pump because it significantly reduced stress responses under tested conditions.

In Malaysia, ASP has been used for flood mitigation because of its ability to remove large volumes of excess water from flood-prone areas. ASP stations are classified as a structural measure under Integrated Flood Management (IFM) approaches implemented by the Department of Irrigation and Drainage [6]. To ensure that the pumping station can discharge floodwater effectively, the ASP should be designed for high hydraulic performance so it can run at an optimal level. Low hydraulic performance of the ASP will increase energy consumption and contribute to higher operating cost for discharging water from flood-prone areas.

The hydraulic performance of ASP is measured based on efficiency, which is the ratio of hydraulic power to the required shaft power. Various geometric and operational parameters have been found to affect the hydraulic performance of ASP. The geometric parameters of ASP include the outer diameter D_o, inner diameter D_i, pitch S, number of flights (or blades) N, screw length L, gap width Gw, and inclination angle β. The operating parameters of ASP include the lifting head, upper water level (h_U), lower water levels (h_L), bucket water level (Z_{wl}), and rotation speed (ω) [1,7].

The ASP efficiency typically ranges between 65% and 75% depending on the size of the screw diameter [8]. Large screw diameters reach approximately 75% efficiency, more than small diameter screw with an efficiency of 65% [9]. The efficiency of ASP could reach 85% if the screw geometry parameter is optimized and designed meticulously [10]. Lyons et al. [11] experimentally investigated the efficiency of a laboratory-scale ASP at different inlet basin water levels and rotational speeds. In their study, optimal efficiency was achieved when operated at approximately 80% of the lower basin level. Chan et al. [12] examined ASP efficiency through a series of CFD simulations considering inclination angle, rotational speed, and number of flights and found that the maximum efficiency was 24.04% obtained by single-flight operation at a 20° and 40 rpm. Nagel [1] mentioned that a single-flight screw could deliver about 64% and a double-flight screw about 80% efficiency. According to a theoretical analysis [13], the additional flight could increase the efficiency of ASP. However, others recommend that two or three flights [14] with single-flight configuration yield the highest performance [8]. In another aspect, lower inclination angles often correspond to a longer screw which results in high flow rates and efficiencies but increases the cost of the installation [14]. According to Muysken [7], the inclination angle used for screw pumps can vary from 26° to 40°, and the most typical inclination angles are around 30°, 35°, and 38°. Nagel [1] generally recommends an operating inclination angle of 30°. In terms of rotational speed, both Nagel [1] and Muysken [7] suggested that the rotational speed of ASP may run from 15 to 60 rpm. Nagel [1] recommended using Muysken's [7] rotational speed as the maximum speed as a function of the outer diameter. For example, a screw with an outer diameter of 1 m should have a maximum rotational velocity of 50 rpm [13]. The fill height gradient in the bucket is also known to impact flow rate due to a small gap between the screw flight and the trough. Recent experiment on the fill height gradient found that the variation in fill height in the bucket was greater at low rotational speed, and the different water level in each bucket along the screw was reduced due to leakage as the bucket translated up to the outlet [15,16].

Design and operation guidance is available through classical handbooks [1,7], while more recent hydraulic engineering literature has documented ASP performance and operational behavior under controlled laboratory conditions [9,11]. The current empirical guidelines [9,11] help in designing ASP but not at an optimal level. It is also important that improving design and operation rules requires knowing why performance changes with operating conditions. However, these mechanisms are difficult to quantify experimentally, and the inability to observe internal bucket dynamics is a limiting factor in model development. Therefore, numerical investigation using CFD offers a pathway to examine internal flow

patterns that are difficult to measure experimentally and to test operating conditions efficiently. CFD has been widely used to investigate the hydraulic performance of Archimedes screw turbine (AST) [17-20], yet validated CFD models of ASP remain limited and underexplored. Simmons et al. [9] were perhaps the first to introduce a validated CFD model for ASP to evaluate the performance of rotational speed at various screw sizes. Later, Chan et al. [12] used CFD to investigate the performance of ASP under various numbers of flights and rotational speeds, but without experimental validation.

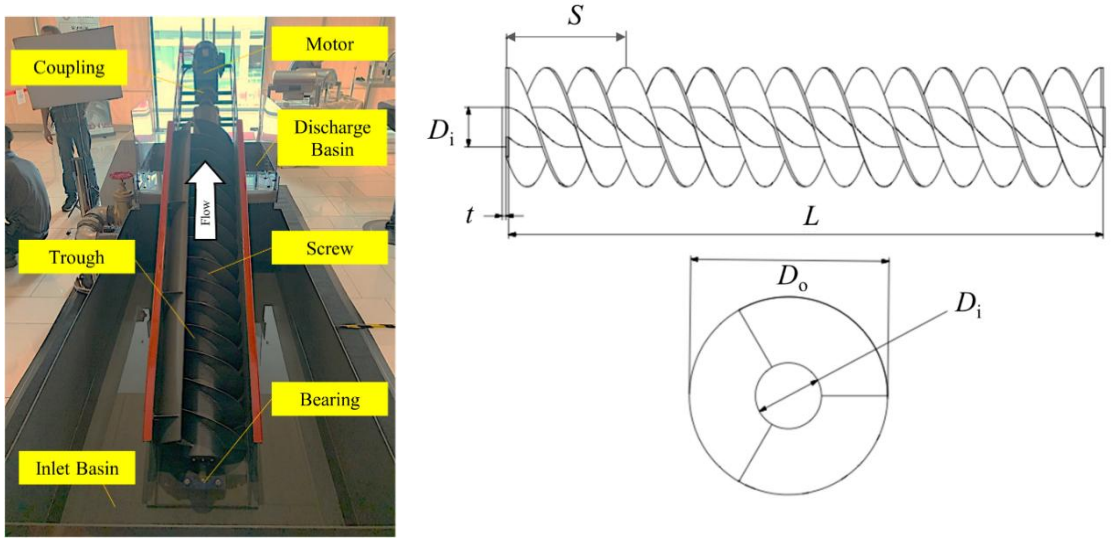
Consequently, there is a need to generate more numerical data and gain a deeper understanding to optimize ASP performance through simulation, where experimental data is lacking. This study aims to develop a CFD model of the ASP and use it to simulate fluid flow at various inclination angles and rotational speeds to identify its peak efficiency. Experimental testing is also conducted, and the data are used to validate the CFD model, ensuring the data are accurate and reliable for use as a guide in engineering design. Findings of this study will help bridge gaps in ASP design to achieve superior hydraulic performance and provide a clearer understanding of the internal flow dynamics across the screw flights.

2. METHODOLOGY

2.1 Experimental setup

The experiment was carried out on a laboratory-scale ASP at a rotational speed of 100 rpm and an inclination angle of 30°, with the flow rate being recorded. However, due to equipment limitations, the experiment was performed under fixed operating and geometrical conditions. Consequently, the experimental data were used to develop a reliable and validated CFD simulation. Based on Figure 1(a), the laboratory-scale ASP consisted of several components, such as a screw, trough, bearings, coupling, and motor, that work together to transport water from a lower to a higher elevation. The screw was made of mild steel, and bearings were mounted at both ends of the screw to support the load and reduce vibration. The screw was driven by a motor and connected by a coupling to allow power to be transmitted effectively. Water from the inlet basin flowed into the screw and the trough was lifted upward to the discharge basin due to the rotating motion of the screw. Figure 1(b) shows the detailed geometric dimensional information of the screw, which includes critical parameters for hydraulic performance. The laboratory-scale ASP was designed with three flights, a length of 1500 mm, an outer diameter of 300 mm, a pitch length of 300 mm, a flight thickness of 10 mm, a gap width of 5 mm, and other detailed specifications as shown in Table 1.

The flow rate of the laboratory-scale ASP was measured using sensorless flow rate technology, which controls and estimates flow without a physical flow meter. This technology features an advanced algorithm that analyses motor speed, power consumption, and system characteristics with an accuracy of ±2%. The system recorded an ASP flow rate of 10.76 L/s. To validate these readings, a preliminary investigation was conducted by calculating the flow rate based on the total volume and the time required to fill the discharge basin. The discharge basin dimensions were 0.79 m (width) × 0.245 m (height) × 0.788 m (length) with a total volume of 0.153 m^3 that was fully filled within 14.9 seconds. Thus, the calculated volumetric flow rate was 0.0102 m^3/s (10.2 L/s), which proved that the test equipment is accurate and reliable for estimating the pump's flow rate.



(a) (b)

Fig. 1. (a) Laboratory-scale ASP and (b) Detailed geometric dimensions of the screw

Table 1. Detailed dimensional specifications of ASP

Parameter	Value	Unit
Inner diameter, D_i	100	mm
Outer diameter, D_o	300	mm
Length, L	1500	mm
Pitch length, S	300	mm
Flight thickness, t	10	mm
Gap width, Gw	5	mm
Touch point, TP	15	mm
Filling point, FP	200	mm
Chute point, CP	590	mm
Hydraulic head, H	569	mm
Motor power, P_m	0.2	kW

2.2 CFD setup

A validated CFD model of the ASP was developed using ANSYS Fluent to replicate the actual performance of a laboratory-scale ASP and monitor its hydraulic performance through a series of simulations at various rotational speeds and inclination angles. For a realistic representation of the flow domain for CFD analysis, the model consisted of two regions; a stationary domain (the trough, inlet, and outlet) and a rotating domain (the screw). Figure 2 illustrates the defined boundary conditions to ensure they provide realistic flow behaviour during simulation. For the inlet boundary, it was specified as a velocity inlet of 0.1 m/s and the outlet boundary was set as a pressure outlet with zero-gauge pressure, allowing the fluid to exit the domain at atmospheric pressure. All walls of the screw and trough were treated as no-slip

walls while the rotating region of the screw was defined using the sliding mesh technique with a specified rotational speed.

The meshing process was carried out to discretize the fluid domain into small finite volume elements, particularly around the helical flights and the narrow clearance space between the screw and the trough. In this study, polyhedral mesh was employed to ensure solver stability and suitability for curved surfaces. Additionally, inflation layers were applied over wall surfaces of the screw flight and trough to accurately capture flow behaviour and to resolve boundary layer effects, as shown in Figure 3. For accurate results and to prevent convergence issues during simulation, the maximum skewness and minimum orthogonality quality were strictly maintained below 0.9 and above 0.1, respectively, throughout the mesh generation process.

In this study, the k-ε turbulence model was used to simulate the turbulent flow of ASP to balance computational cost and predictive capability. Accordingly, a turbulent flow was assumed for the simulation. This phenomenon can be proven by estimating the Reynolds number for bulk flow in the passage, assuming the flow passage in the screw as an annular flow region with an outer diameter of 0.3 m and an inner diameter of 0.1 m. As per our experimental data, the flow rate was 10.76 L/s. So, using standard fluid properties, this condition corresponded to a Reynolds number of approximately 34,100, exceeding the conventional turbulent flow criterion for open channel flow, which indicated that inertial forces dominate viscous effects. It is also worth noting that the free surface flow in an Archimedes screw pump was geometrically complex, unsteady, and mostly turbulent. Such characteristics has led Simmons et al. [9] to utilize a turbulence model in their simulation.

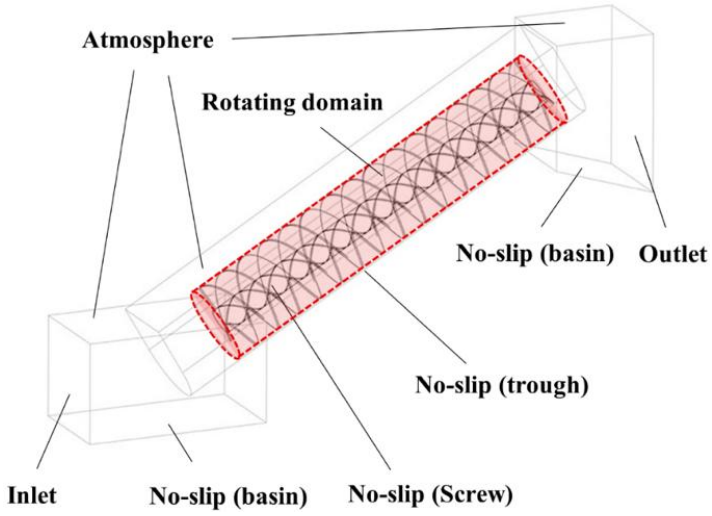


Fig. 2. Boundary conditions of CFD model of ASP

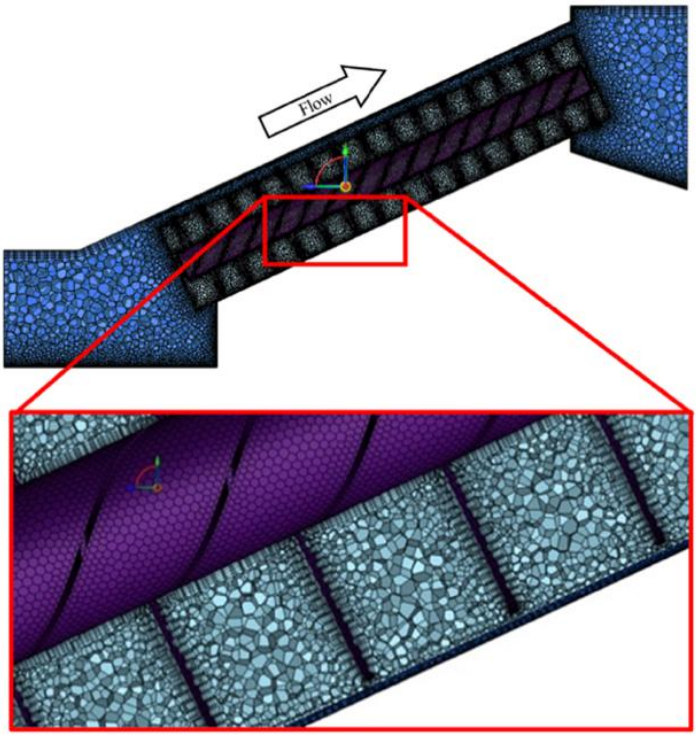


Fig. 3. Computational domain meshed with polyhedral cells

For the multiphase model, the Volume of Fluid (VOF) method was employed to simulate incompressible flow involving two immiscible phases, namely water and air [21]. The Semi-Implicit Method for Pressure-Linked Equations (SIMPLE) algorithm was employed for pressure–velocity coupling as this scheme is widely used in transient and steady-state simulations for its robustness and efficiency in solving incompressible flow problems. For pressure interpolation, the Pressure Staggering Option (PRESTO!) scheme was selected as it is particularly suitable for flows involving strong body forces, swirling flows, and rotating domains [22]. This study used a fully implicit scheme, with a convergence criterion of 10^{-5} to monitor solution convergence. A fixed time step size of 0.0016 seconds was used for the transient simulation with a sufficient number of time steps and iterations. For instance, a simulation at 100 rpm using this time step size yields 1° angular displacement per time step. Therefore, to reach a steady-state flow at 8 seconds requires a total of 4,800 time steps. A series of simulations of the ASP at various inclination angles (20°, 25°, and 30°) and rotational speeds (25, 50, 75, and 100 rpm) were performed, and the outputs were monitored in terms of water flow rate and screw torque, which serve as the key performance indicators of efficiency. The variables were selected within the typical operating ranges reported in previous studies [7]. The screw configuration at the different inclination angles considered in this study is illustrated in Figure 4. The figure also indicates the hydraulic head at different inclination angles.

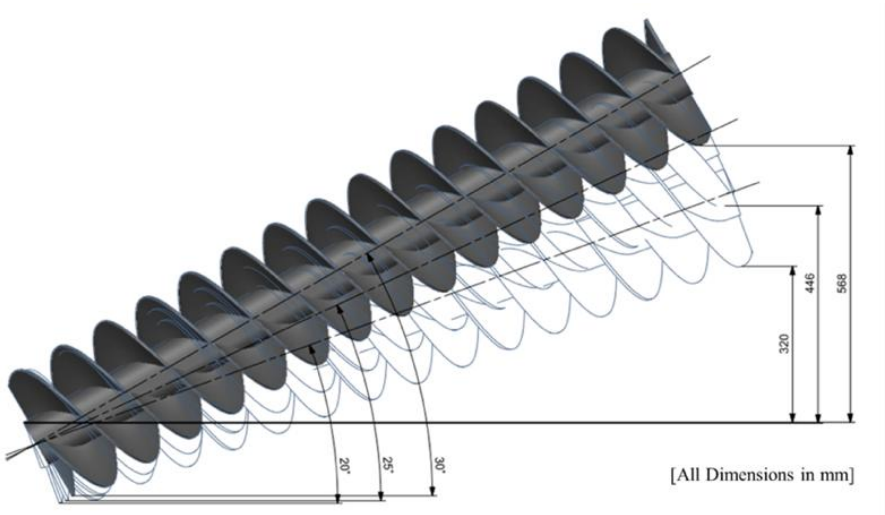


Fig. 4. Configurations of the ASP screw at different inclination angles

In a rotating system such as ASP, the mechanical power can be calculated using Equation (1),

$$P_m = T\omega \quad \text{(W)} \tag{1}$$

where T (Nm) is the torque of the screw while ω (radians per second) is the angular velocity of the rotating screw. Hydraulic power refers to the rate of useful work performed by the screw to lift a certain volume of fluid. The hydraulic power can be calculated using Equation (2),

$$P_h = \rho g Q H \quad \text{(W)} \tag{2}$$

where ρ (kg/m^3) is the density of the fluid, g (m/s^2) is the gravitational force, Q (m^3/s) is the volume flow rate, and H (m) is the hydraulic head. After obtaining the mechanical power and hydraulic power, the hydraulic efficiency can be determined using the following Equation (3),

$$\eta = \frac{P_h}{P_m} \quad \text{(-)} \tag{3}$$

2.3 Mesh independence study

To verify the accuracy and reliability of the numerical results, a mesh independence study was performed. The ASP model was meshed at four different levels of refinement, and the sensitivity of the results to mesh resolution was evaluated before proceeding to simulation at various rotational speeds and inclination angles. Figure 5 shows the flow rate across various mesh resolutions, and it was found that the flow rate reached a steady value of 10.43 L/s for the mesh with 1,347,440 cells, having a maximum skewness of 0.69 and a minimum orthogonal quality of 0.12. Hence, this mesh was selected to perform the remaining simulations and analysis.

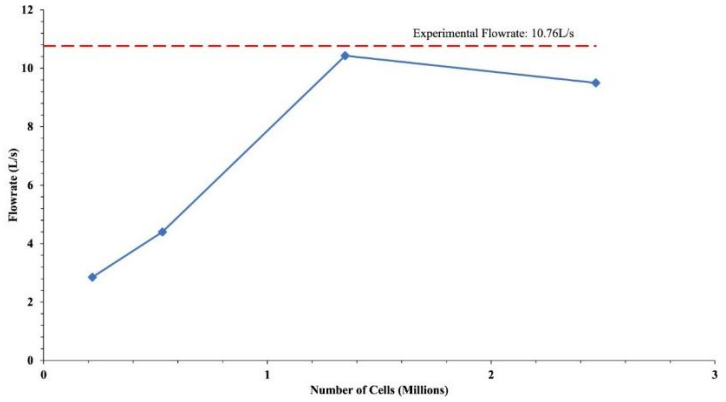


Fig. 5. Results of mesh independence study

3. RESULTS AND DISCUSSION

3.1 CFD validation

Experimental data of laboratory-scale ASP was recorded at 10.76 L/s of water flow rate to the outlet basin at an inclination angle of 30° and an operation rotational speed of 100 rpm. The CFD simulation produced a corresponding outlet flow rate of 10.43 L/s. The constant flow rate was generated after the flow achieved a steady-state condition, which was about 6 sec of flow time, as illustrated in Figure 6. The CFD predictions showed good agreement with the experimental measurements, with a percentage error of approximately 3.07% or a difference of 0.33 L/s.

Figure 7 demonstrates the visual representation of the water volume fraction at the mid-plane of the ASP model through time. The two phases are color-coded, where blue regions represent air and red regions represent water. Figure 7(a) illustrates the initial state of the ASP at flow time = 0 s before the simulation runs, where water is defined at the inlet basin. Figure 7(b) illustrates the steady-state condition of the ASP at flow time > 8 s. Here, water is continuously transported from the inlet basin to the discharge basin.

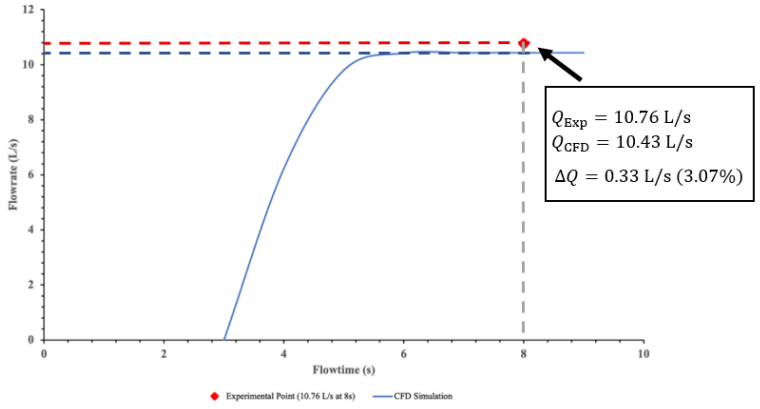


Fig. 6. Comparison of flow rate between CFD simulation and experimental data

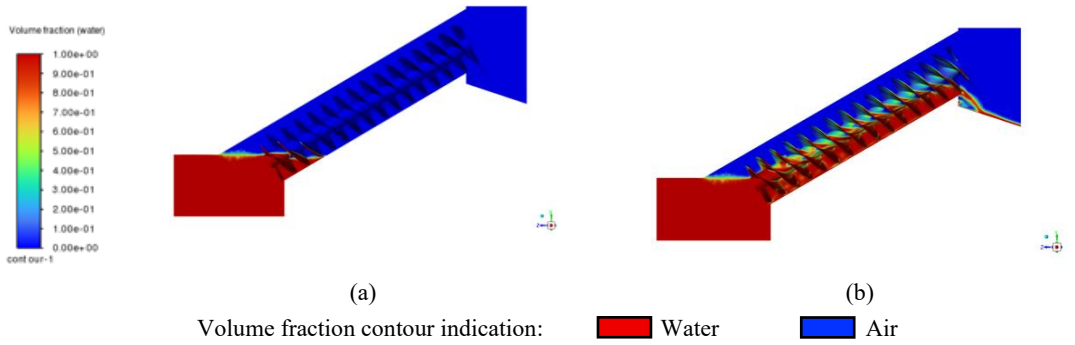


Fig. 7. Water volume fraction at mid-section of ASP at (a) initial (flow time = 0 s) and at (b) steady state (flow time > 8 s)

3.2 Hydraulic performance

The hydraulic performance of the laboratory-scale ASP was evaluated through a series of simulations at various rotational speeds and inclination angles. These simulations aim to identify the optimal rotational speed and inclination angle to achieve peak efficiency of ASP. Figure 8 shows the variation of flow rate with rotational speed at different inclination angles. Based on Figure 8, the flow rate increased proportionally with the rotational speed at all inclination angles. At an inclination angle of 20°, the flow rate increased from 2.9 L/s at 25 rpm to 12.68 L/s at 100 rpm. Similar increasing trends were observed at inclination angles of 25° and 30°. This situation aligns with the principle that a higher rotational speed increases the volume of water because a screw transports more fluid upwards per rotation within a given unit of time at higher rotational speed. However, flow rate becomes less significant at 75 rpm indicating the beginning of hydraulic losses due to increased turbulence and partial backflow within the screw channel. Also, flow rate was observed to decrease as the inclination angle was increased at the same rotational speed influenced by higher gravitational resistance and a reduction in volume caused by leakage at the gap. Conversely, a lower inclination angle allows for the transport of a greater volume of water at the same rotational speed.

Torque is generated by the hydrostatic pressure exerted by the weight of the water or buckets on the surface of the helical flights. Figure 9 illustrates the variation of torque with rotational speed at different inclination angles. Based on Figure 9, torque increases moderately as rotational speed and inclination angle increase. At a 30° inclination angle, torque rises from 5.8 N·m to 7.75 N·m due to higher rotational speed causing high friction and fluid shear forces on the helical flight surface, which requires greater torque to overcome the resistance. However, the influence of rotational speed on torque magnitude is less dominant compared to inclination angle.

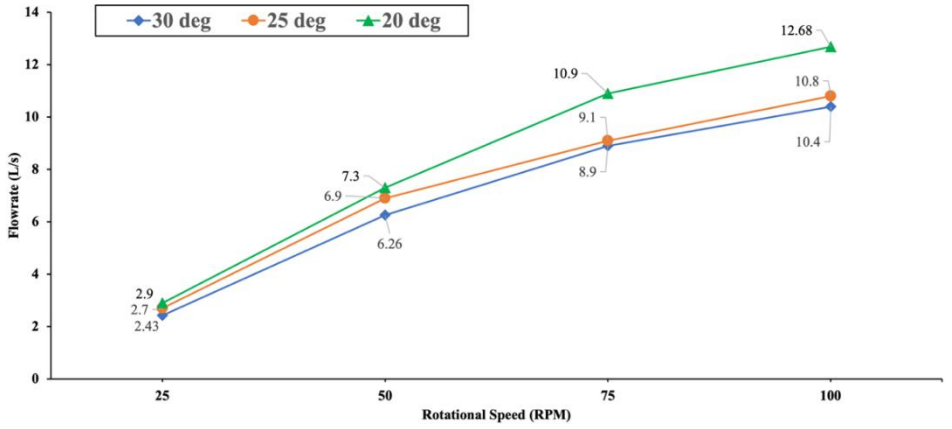


Fig. 8. Variation of flow rate with rotational speed at different inclination angles

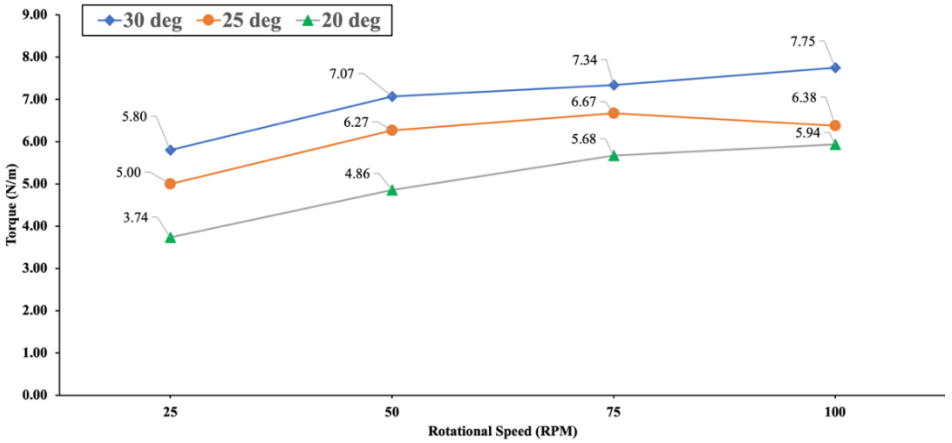


Fig. 9. Variation of torque with rotational speed at different inclination angles

Figure 10 illustrates the overall efficiency of the laboratory-scale ASP at various rotational speeds and inclination angles. The highest efficiency of 94.4% was recorded at a speed of 50 rpm and an inclination angle of 30°. A downward trend in efficiency was observed at higher speeds. Across all inclination angles, the peak efficiency was recorded at 90.15%, 91.96%, and 94.40% at 20°, 25°, and 30°, respectively. These findings are consistent with the data reported by Simmons et al. [9], which indicated that the highest efficiency for laboratory-scale ASPs occurs within a rotational speed range of 30 to 50 rpm. As the rotational speed increased, the overall efficiency declined due to water friction against the helical screw and leakage through the clearance gaps. These results demonstrate that optimal ASP operation is achieved at moderate screw rotation speeds to balance energy consumption with flow generation.

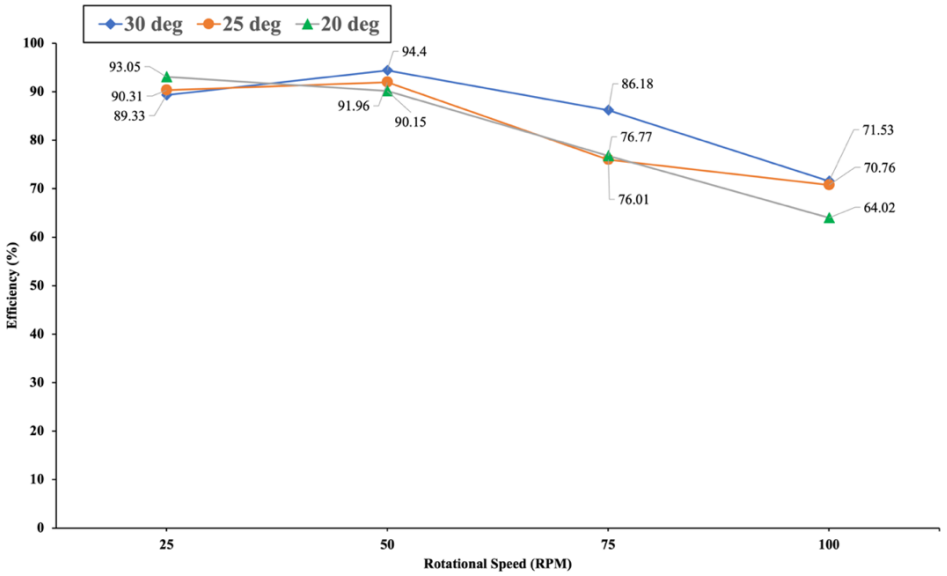


Fig. 10. Overall efficiency variation with rotational speed at different inclination angles

3.3 Flow fields

CFD enables a detailed analysis to identify water flow behavior within the screw and regions that are difficult to capture during experimental measurements. From the simulation, water volume fraction, wall shear stress, and velocity field were extracted to investigate flow development and energy loss mechanisms in the region between the screw and the trough. Figure 11 represents the contours of mid-plane water volume fraction at various rotational speeds and inclination angles. Based on the contour, there was a thinning layer near the gap clearance due to gap leakage. Also, the bucket at the bottom remained filled while upper buckets gradually lost water due to clearance leakage, gravity, and reduced hydrostatic support [9,10] at higher rotational speeds or lower inclination angles. Although there was some leakage at the clearance space, it became significant when the flow was insufficient to keep the bucket constantly full. Overall, the numerical model accurately captures free-surface behaviour inside the screw and provides clear insight into how water leakage could reduce the performance.

Figure 12 illustrates the wall shear stress contours on the screw surface. At a rotational speed of 100 rpm, wall shear stress developed near the flight tip and became more pronounced at low inclination angles due to centrifugal forces displacing water to intensifies the fluid's resistance against the flight surfaces and triggers turbulent motion, causing higher energy dissipation. Conversely, lower wall shear stress occurred at moderate rotational speeds, where frictional losses were minimized. Observations of the wall shear stress contours on the flight surface confirmed fluid movement across the helical screw surface resulting from increased flow on the helical flight surface due to high relative velocity between water and flight, leading to an increase in wall shear stress. Figure 13 shows water velocity contours at mid-plane channel, showing stable transport of water along the screw. Based on the observation, higher velocities near the discharge zone are due to flow acceleration results from changes in geometry and boundary conditions. Velocities increased along the screw channel particularly at the free surface and flight edges due to high rotational speed which contributed to shear effects on the helical flight and potential energy loss. A uniform

distribution was observed at the low-velocity setup which resulted in low losses and effective flow conveyance. To reduce losses and improve efficiency, it is necessary to identify low-velocity zones near the interface between the screw and the trough to indicate any recirculation or flow slippage.

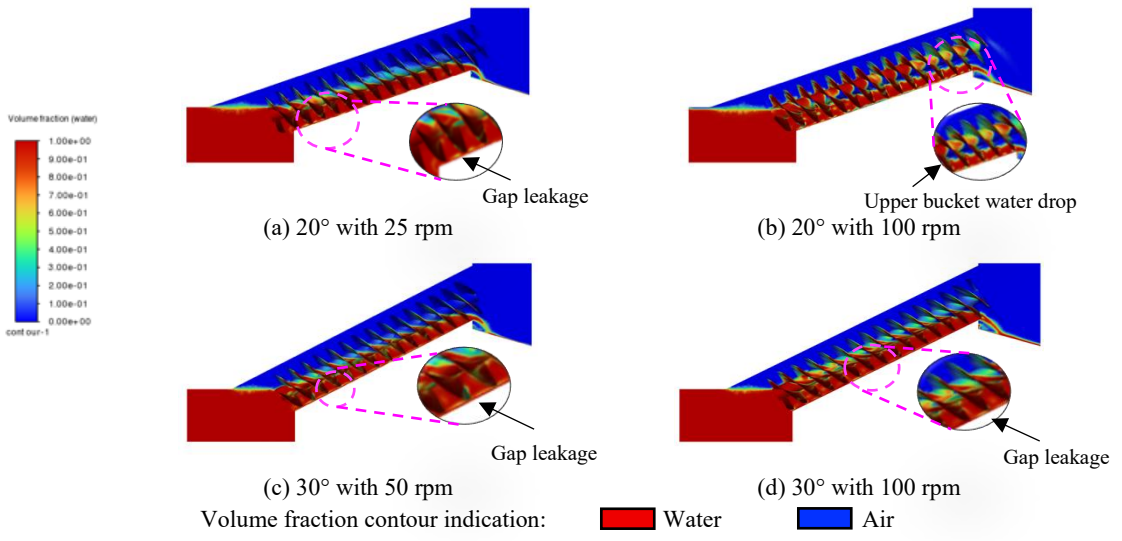


Fig. 11. Contours of mid-plane water volume fraction at (a) 20° with 25 rpm, (b) 20° with 100 rpm, (c) 30° with 50 rpm, and (d) 30° with 100 rpm

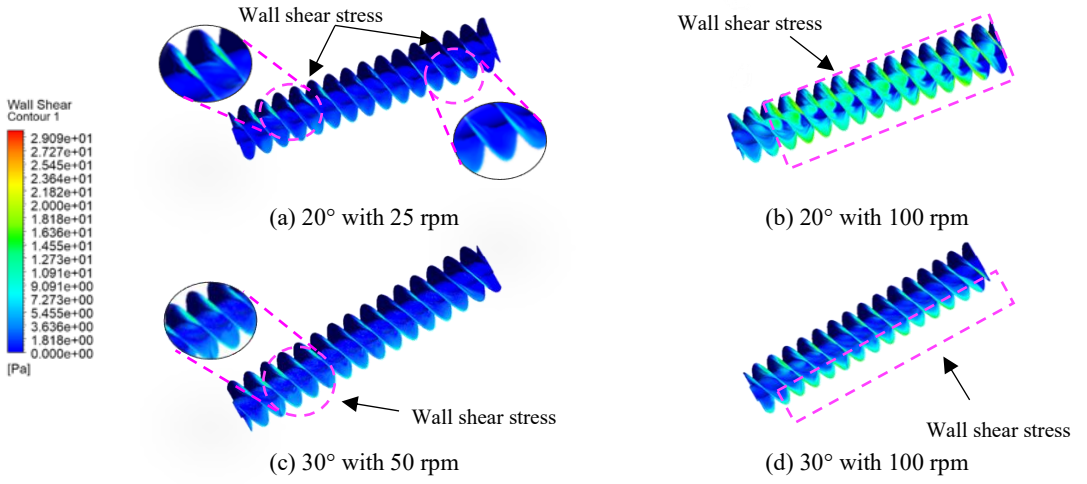


Fig. 12. Contours of wall shear stress on ASP at (a) 20° with 25 rpm, (b) 20° with 100 rpm, (c) 30° with 50 rpm, and (d) 30° with 100 rpm

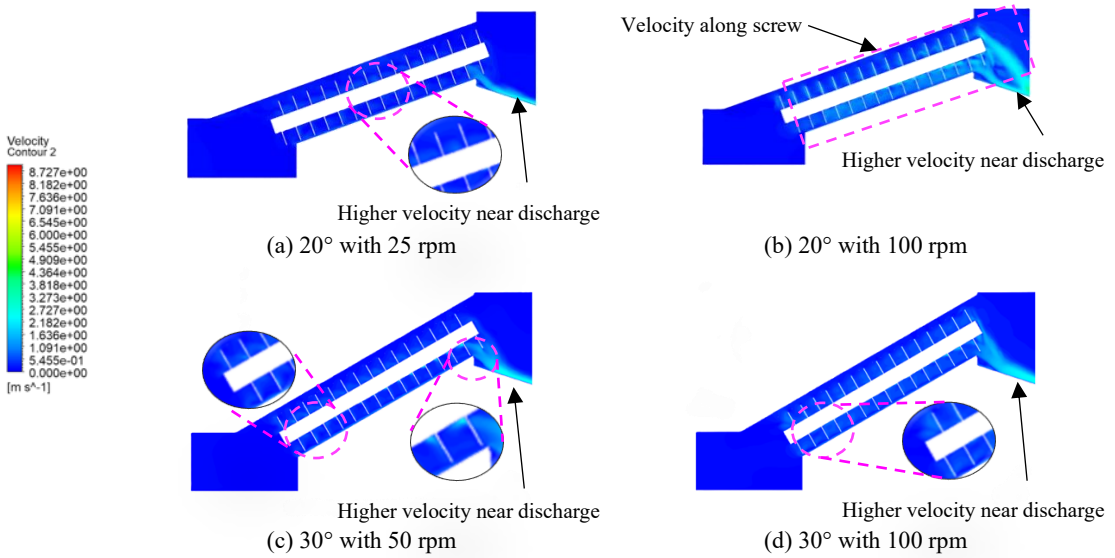


Fig. 13. Contours of mid-plane velocity at (a) 20° with 25 rpm, (b) 20° with 100 rpm, (c) 30° with 50 rpm, and (d) 30° with 100 rpm

4. CONCLUSIONS

This study has successfully developed and validated a CFD model of ASP against experimental data to evaluate the hydraulic performance and internal flow dynamics of a laboratory-scale ASP through a series of CFD simulations at various inclination angles and rotational speeds. Based on the simulation data, the ASP achieved optimal hydraulic performance at 50 rpm rotational speed and a 30° inclination angle with the highest efficiency of 94.40%. However, beyond 50 rpm, the efficiency began to decline due to friction, overflow spillage, and leakage at the clearance gap between the screw and the trough. These findings provide insight into the internal bucket dynamics of the screw and reliable operational limits to optimize energy efficiency and the discharge capacity of the ASP, specifically to help engineers design optimal performance of ASP to effectively transfer large volumes of excess water. There are several limitations worth acknowledging to enhance the hydraulic performance of ASP. First, this study investigated only one operating parameter (that is, rotational speed) and one installation/orientation parameter (that is, inclination angle), while the geometric parameters of the screw were kept constant. Second, the optimum condition and orientation identified in this study were determined from the limited conditions rather than through a systematic optimization procedure. Third, the experiment was conducted using a laboratory-scale ASP under a single operating condition. Therefore, future studies should consider systematic optimization methods that incorporate a wider range of parameters to accurately determine the optimal configuration of the ASP. Future work should also focus on modifying the existing experimental rig so that the pump performance can be evaluated across various operating conditions and scales, and the resulting data will then be used to validate CFD predictions under corresponding operating conditions and scales.

5. ACKNOWLEDGEMENTS/FUNDING

The work was not funded by any research grant.

6. CONFLICT OF INTEREST STATEMENT

The authors declare that they have no known competing financial interests or personal relationships that could have appeared to influence the work reported in this paper.

7. AUTHORS' CONTRIBUTIONS

Nelson Lee Teck Hua: Data curation, formal analysis, investigation, methodology, validation, writing – original draft;

Muhammad Noor Afiq Witri Muhammad Yazid: Supervision, conceptualisation, writing - review & editing;

Muhammed Amirul Asyraf Hasnan: Writing - review & editing, resources.

8. DECLARATION OF GENERATIVE AI IN THE WRITING PROCESS

During the preparation of this work, the authors used Google Gemini for language editing and proofreading. After using this tool/service, the authors reviewed and edited the content as needed and take full responsibility for the content of the publication.

9. DATA AVAILABILITY/SUPPLEMENTARY MATERIALS

The datasets used and/or analysed during the current study are available from the corresponding author on reasonable request.

10. ETHICS STATEMENT

The authors declare that this research did not involve human or animal subjects. All experimental procedures were performed following the institutional Safety, Health, and Environmental (HSE) protocols of Universiti Teknologi Malaysia (UTM).

11. REFERENCES

[1] G. Nagel, Archimedian screw pump handbook: Fundamental aspects of the design and operation of water pumping installations using Archimedian screw pumps, RITZ-Pumpenfabrik OHG, 1968.

[2] T. L. Heath, Ed., Archimedes. The works of Archimedes: Edited in Modern Notation with Introductory Chapters. Cambridge University Press, 2009.

[3] J. P. Hoffstaedt *et al.*, "Low-head pumped hydro storage: A review of applicable technologies for design, grid integration, control and modelling," *Renewable and Sustainable Energy Reviews*, vol. 158, pp. 112119, 2022. doi: 10.1016/j.rser.2022.112119

[4] A. Koenig, "Introduction of the Archimedean screw pump to East Asia during the seventeenth and eighteenth centuries," *Chinese Annals of History of Science and Technology*, vol. 4, no. 1, pp. 102 - 138, 2020.

[5] Á. De La Llave-Propín *et al*., "Archimedes' screw helps optimize fish catching, welfare and product quality," *Aquaculture*, vol. 612, pp. 743067, 2026, doi: 10.1016/j.aquaculture.2025.743067.

[6] Department of Irrigation and Drainage, "*Flood Management - Programme and Activities*," [Online]. Available: https://www.water.gov.my/index.php/pages/view/419. [Accessed September 01, 2026].

[7] J. Muysken, "Berekening van het nuttig effect van de vijzel," *Ing.*, vol. 21, pp. 77 – 91, 1932.

[8] J. Wijdieks, and M. G. Bos, "Pumps and pumping stations", in *Drainage principles and applications*, H. P. Ritzema, Ed. Wageningen: International Institute for Land Reclamation and Improvement, pp. 965–999, 1994.

[9] S. C. Simmons *et al.*, "Development of a computational fluid dynamics model for Archimedes screw pumps," In *Canadian Society of Civil Engineering Annual Conference,* Cham: Springer Nature, Switzerland, 2023, pp. 215 – 235, doi: 10.1007/978-3-031-61519-1_16

[10] S. C. Simmons and W. D. Lubitz, "Analysis of internal fluid motion in an Archimedes screw using computational fluid mechanics," *Journal of Hydraulic Research*, vol. 59, no. 6, pp. 932 – 946, 2021, doi: 10.1080/00221686.2020.1844813.

[11] M. Lyons, *et al.*, "Experimental investigation of Archimedes screw pump," *Journal of Hydraulic Engineering*, vol. 146, no. 8, pp. 04020057, 2020, doi: 10.1061/(asce)hy.1943-7900.0001786.

[12] W. L. Chan, U. K. Jamaludin, and N. S. Azahari, "Archimedes screw pump efficiency based on three design parameters using computational fluid dynamics software – Ansys CFX", *Journal of Physics Conference Series*, vol. 2688, no. 1, pp. 012015, 2024, doi: 10.1088/1742-6596/2688/1/012015.

[13] C. Rorres, "The turn of the screw: Optimal design of an Archimedes screw", *Journal of Hydraulic Engineering*, vol. 126, no. 1, pp. 72 – 80, 2000, doi: 10.1061/(asce)0733-9429(2000)126:1(72).

[14] S. C. Simmons, L. Miller, and W. D. Lubitz, "Review and evaluation of Archimedes screw pump design guidance," In *Symposium on Responsible Engineering and Living*. Cham: Springer International Publishing, 2022, pp. 225-243.

[15] S. C. Simmons, A. Dorier, C. E. Mendes, G. Dellinger, and W. D. Lubitz, "Experimental study of gap leakage in archimedes screw pumps," in *Proceedings of the Canadian Society for Civil Engineering Annual Conference*, Springer, Cham, 2025, pp. 385–399, doi: 10.1007/978-3-031-95107-7_32.

[16] S. C. Simmons, C. E. Mendes, and W. D. Lubitz, "Modelling the fill height gradient in Archimedes screw pumps," *Journal of Hydraulic Research*, pp. 718-727, 2026, doi: 10.1080/00221686.2026.2692576.

[17] G. Dellinger *et al.*, "Effect of slope and number of blades on Archimedes screw generator power output," *Renewable Energy*, vol. 136, pp. 896-908, 2019, doi: 10.1016/j.renene.2019.01.060

[18] K. Shahverdi, *et al.*, "CFD numerical simulation of Archimedes screw turbine with power output analysis," *Ocean Engineering*, vol. 231, pp. 108718, 2021, doi: 10.1016/j.oceaneng.2021.108718

[19] Z. Abbas, *et al.*, "Numerical and experimental investigation of an Archimedes screw turbine for open channel water flow application," *Energy Science & Engineering*, vol. 12, no. 4, pp. 1317 - 1336, 2024, doi: 10.1002/ese3.1649

[20] H. B. Lamesgin and A. N. Ali, "Optimization of screw turbine design parameters to improve the power output and efficiency of micro-hydropower generation," *Cogent Engineering*, vol. 11, no. 1, pp. 2327906, 2024, doi: 10.1080/23311916.2024.2327906

[21] A. Abdullah, G. M. U. Din, T. Sultan, M. Aleem, and M. S. Shazil, "VOF-based simulation of turbulent air-water flow over gravel beds in open channels," *Fluid Dynamics & Materials Processing*, vol. 22, no. 3, pp. 1–10, 2026, doi: 10.32604/fdmp.2026.077023.

[22] ANSYS Fluent, Ansys Fluent user's guide. ANSYS Inc., 2026.

© 2026 by the authors. Submitted for possible open access publication under the terms and conditions of the Creative Commons Attribution (CC BY-NC-ND) license (http://creativecommons.org/licenses/by/4.0/).